Journal of Hydrology 603 (2021) 127022

Contents lists available at ScienceDirect

Journal of Hydrology

journal homepage: www.elsevier.com/locate/jhydrol

Real-time assessment of flash flood impacts at pan-European scale: The ReAFFINE method

Josias Ritter *, Marc Berenguer, Shinju Park, Daniel Sempere-Torres

Center of Applied Research in Hydrometeorology, Universitat Politècnica de Catalunya, BarcelonaTech, Jordi Girona 1-3 (C4-S1), 08034 Barcelona, Spain

ARTICLE INFO

This manuscript was handled by Marco Borga, Editor-in-Chief, with the assistance of Nadav Peleg, Associate Editor

Keywords:
Flash flood
Impact forecasting
Early warning
Radar rainfall
Continental scale

ABSTRACT

The development of early warning systems (EWSs) is a key element for the effective mitigation of flash flood impacts. Emergency managers and other end-users increasingly recognise the benefit of tools that automatically translate the forecasted flash flood hazard (e.g. expressed in terms of peak discharge or return period) into the expected socio-economic impacts (e.g. the affected population). While previous studies aimed at forecasting flash flood impacts at local or regional scales, this paper presents a simple approach for estimating in real time the flash flood impacts at pan-European scale. The proposed method – named ReAFFINE – is designed to be integrated into an EWS for end-users operating over large spatial domains (e.g. across regions or countries). ReAFFINE uses the pan-European flash flood hazard estimates from the ERICHA system to retrieve the potentially flooded areas from the national flood maps (generated in the framework of the EU Floods Directive). By combining the potentially flooded areas with socio-economic exposure information, ReAFFINE estimates in real time the exposed population and critical infrastructures. For two catastrophic flash flood events affecting Europe in recent years, ReAFFINE has demonstrated the capability to identify impacts over large spatial scales. Also at sub-regional level, the method has mostly been able to locate the areas and municipalities where the most important impacts occurred. The results also show that the performance is sensitive to the quality of the rainfall estimates that drive the hazard estimation, and to the comprehensiveness of the employed flood maps.

1. Introduction

Flash floods (FFs hereafter) are one of the most devastating natural hazards in Europe, causing numerous casualties (Barredo, 2007; Petrucci et al., 2019; Terti et al., 2017) and tremendous economic losses (EEA, 2010; Gaume et al., 2009; Munich Re, 2017; Paprotny et al., 2018). This type of flooding is characterized by intense downpours in small to medium-sized, often mountainous catchments, leading to a short response time between the rainfall and the discharge peak in the stream network (in the range of minutes to a few hours). The sudden event onset often hinders a timely flood response (e.g. in form of evacuations or road closures) and is the main reason for the high socio-economic impacts caused by FFs (EEA, 2010; Sene, 2013; Spitalar et al., 2014). Early warning systems (EWSs) aim to extend the time span available for applying flood response measures and are therefore considered to bear the highest potential for effectively reducing FF impacts (EEA, 2010).

The Sendai Framework for Disaster Risk Reduction (UNISDR, 2015a) demands a leap in the development and availability of EWSs by 2030. Many countries already dispose of FF EWSs that translate (observed and forecasted) rainfall into the expected response in the stream network (i.e. the FF hazard). Real-time and operational examples were demonstrated, for instance, in areas in the United States (Clark et al., 2014; Georgakakos, 2006), Switzerland (Liechti et al., 2013; Zappa et al., 2008), Spain (Corral et al., 2009; Versini et al., 2014), France (Javelle et al., 2010, 2016), and Italy (Corral et al., 2019; Laiolo et al., 2014; Silvestro et al., 2011); for reviews including more examples, see Alfieri et al. (2012, 2019), Gourley et al. (2014), Hapuarachchi et al. (2011), or Li et al. (2018). At European scale, two systems have been delivering for several years FF hazard forecasts to end-users across the continent: ERIC (European Runoff Index based on Climatology; Alfieri and Thielen, 2015; Raynaud et al., 2015) and ERICHA (European Rainfall-InduCed Hazard Assessment; Park et al., 2017, 2019). Both systems compute their warnings by comparing (observed and forecasted) basin-aggregated rainfall to thresholds derived from climatology. ERICHA uses fixed rainfall thresholds, whereas ERIC dynamically updates the thresholds in function of the current catchment conditions (e.g. soil moisture). The two systems are complementary: While ERIC uses

* Corresponding author.
E-mail address: ritter@crahi.upc.edu (J. Ritter).

https://doi.org/10.1016/j.jhydrol.2021.127022
Received 5 April 2021; Received in revised form 5 September 2021; Accepted 27 September 2021
Available online 8 October 2021

numerical weather prediction (NWP) precipitation forecasts as input to assess the FF hazard for the coming five days, the ERICHA system generates high-resolution (1 km and 15 min) warnings for the next few hours using radar-based rainfall observations and nowcasts.

The systems mentioned above predict the hazard component of FFs (expressed e.g. in terms of the peak discharge or return period in the stream network). To estimate the potential impacts of a forecasted FF, it is necessary to combine the hazard forecasts with socio-economic exposure and vulnerability information (e.g. the locations of settlements or critical infrastructures). In the current practice, emergency managers usually do this combination non-automatically and based on personal experience, which is time-consuming and results in subjective decisions (Merz et al., 2020; WMO, 2015). Tools that automatically translate the hazard forecasts into the expected impacts can speed up the decision process and reduce subjectivity, ultimately leading to an improved flood response (Taylor et al., 2018; UNISDR, 2015b).

Prior efforts to automatically forecast FF impacts showed promising results. The existing approaches forecast the impacts in terms of qualitative FF severity levels (Calianno et al., 2013; Saint-Martin et al., 2016), the number of inundated properties (Le Bihan et al., 2017), effects on the road network (Versini et al., 2010; Vincendon et al., 2016), flooded critical infrastructures (Ritter et al., 2020), and affected population and direct economic losses (Ritter et al., 2020; Silvestro et al., 2019). These methods require exposure and vulnerability datasets in very high resolution; as a reference, Ritter et al. (2020) used a resolution of 25 m over the region of Catalonia (Northeast Spain). The real-time application of such high-resolution approaches over larger areas is computationally challenging, which is the main reason why they have been limited to local or regional domains. To today, a method that forecasts FF impacts over large domains (e.g. across regions or countries) does not exist, but it would be beneficial in two ways: Firstly, it would extend the coverage of FF impact forecasts to areas where no such decision support is available yet (e.g. many European countries). Secondly, it would offer a more transboundary perspective on potential FF impacts, which can be useful for end-users operating on the international level, such as transboundary river catchment authorities or the Emergency Response Coordination Centre (ERCC) of the European Union (Emerton et al., 2016; Merz et al., 2020; Thielen et al., 2009; Ward et al., 2015). The European Flood Awareness System (EFAS) already includes a forecast of the impacts of fluvial floods in European catchments larger than 500 km^2 (the Rapid Risk Assessment; Dottori et al., 2017). Complementing this system with a method detecting the impacts of FFs in the smaller basins across Europe would significantly extend the available decision support.

In this work, we build on the FF impact forecasting method ReAFFIRM (Real-time Assessment of Flash Flood Impacts – a Regional high-resolution Method; Ritter et al., 2020) and we propose an approach that is applicable at European scale, named ReAFFINE (Real-time Assessment of Flash Flood Impacts at paN-European scale). The proposed method estimates the potential FF impacts across Europe by complementing hazard simulations from the ERICHA system with components that account for the socio-economic exposure of the areas at risk. ReAFFINE integrates a variety of datasets available throughout the EU (e.g. flood maps or population density maps), which enables a homogeneous impact estimation across borders. The method is adapted to real-time conditions and designed to be integrated into an EWS with pan-European coverage.

The following section 2 provides a detailed description of ReAFFINE, its individual components, and how it has been applied using the available datasets. In section 3, the method is demonstrated on two recent FF events that caused numerous fatalities and widespread economic losses, and the resulting impact estimates are compared to post-event observations from various information sources. Finally, in section 4, we draw some general conclusions and point towards potential future developments.

2. The ReAFFINE method

The objective of this study is to enhance the decision support during FFs for end-users operating over large spatial scales. We propose the method ReAFFINE, which estimates in real time the socio-economic impacts of FFs across Europe. This is achieved through the application of three modules (Fig. 1):

1. The hazard module assesses the FF hazard in real time. For this purpose, we have chosen the ERICHA system (section 2.1) that simulates the FF hazard level along a gridded drainage network over Europe based on radar rainfall observations.
2. The flood map module (section 2.2) transforms the FF hazard levels in the drainage network into hazard levels in the floodplains. In ReAFFINE, this is done based on the national flood maps generated by the Member States through the implementation of the European Floods Directive (European Commission, 2007).
3. The impact assessment module (section 2.3) translates the hazard levels in the floodplains into socio-economic impacts. In ReAFFINE, the impacts are assessed in terms of potentially affected population and critical infrastructures in the floodplains, based on pan-European exposure information.

The following subsections describe the details of the three modules of ReAFFINE, outlining the individual steps of the method and the necessary preprocessing of the employed datasets. An overview of the spatial and temporal resolutions used by the ReAFFINE components is provided in Table 1. In practice, the chain of ReAFFINE modules is triggered every 15 min; i.e. every time new rainfall inputs become available (Fig. 1). On a standard server, the overall computing time from the OPERA radar composites to the impact outputs amounts to about 90 s (Table 1). A such short latency does not significantly delay the transmission of the outputs to the end-user and thus the emergency response.

2.1. Flash flood hazard estimation: The ERICHA system at European scale

For estimating the FF hazard, we have employed the ERICHA system (Corral et al., 2019; Park et al., 2017, 2019), which was implemented in real time at European scale in the framework of the eponymous research project ERICHA (www.crahi.upc.edu/ericha/). Since 2017, the ERICHA FF hazard nowcasts have been displayed on the online platform of the European Flood Awareness System (www.efas.eu/en/flash-flood-indicators), where they have been used for operational decision support by water agencies and emergency services operating at regional, national, and international level.

The ERICHA system generates FF hazard nowcasts for European streams with drainage areas of 5–2 000 km^2. The main dynamic input for the ERICHA system consists of real-time radar rainfall composites from OPERA (Operational Program for the Exchange of weather RAdar information; www.eumetnet.eu/opera). These composites provide precipitation estimates covering all of Europe in high-resolution (2 km, 15 min). From these rainfall estimates, the ERICHA system calculates the basin-aggregated rainfall amounts over a gridded drainage network in 1 km resolution. To determine the FF hazard, the basin-aggregated rainfall amounts are compared to basin-aggregated intensity-duration thresholds adapted from those used by the EUMETNET project Meteoalarm (www.meteoalarm.eu). The result is the estimated hazard level in the drainage network in colour code yellow-orange-red (representing low-medium-high hazard levels; see Fig. 2a for an example).

2.2. Flood map module

The goal of the flood map module is to identify in real time the potentially flooded areas. To achieve this, a connection is created between the FF hazard levels (generated by the ERICHA system;

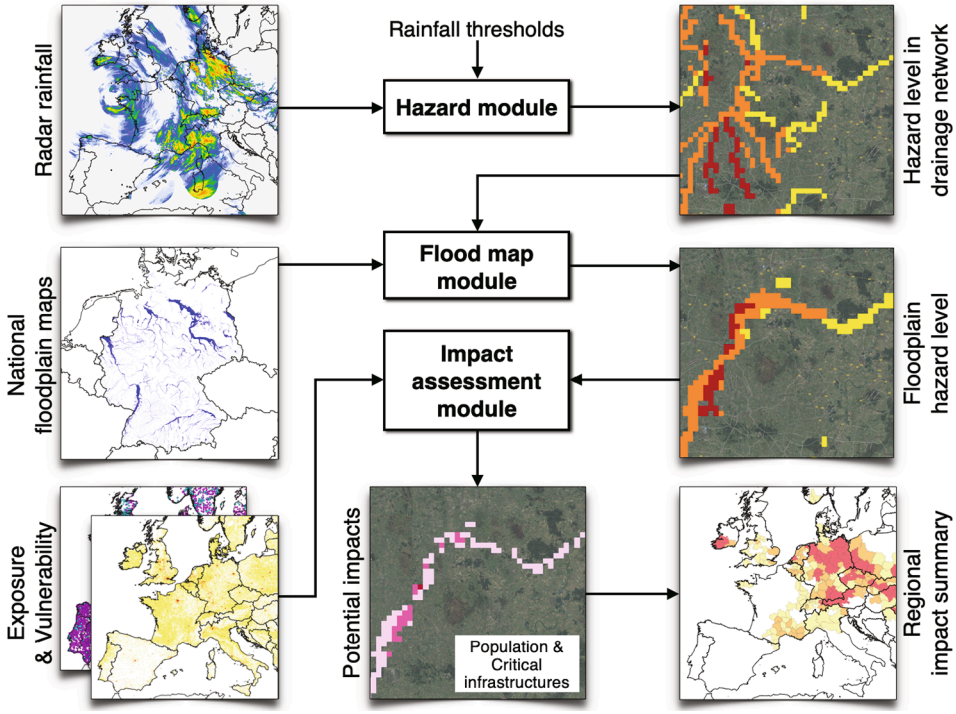

Fig. 1. Concept of the ReAFFINE method.

Table 1
Spatial and temporal resolutions of the ReAFFINE components and their latency for the time step displayed in Fig. 2 and Fig. 4.

Component		Spatial resolution		Execution time step	Latency in real-time operation
		Offline preprocessing	Real-time operation		
OPERA radar rainfall estimation		n/a	2 km	15 min	< 1 s
ERICHA FF hazard module		n/a	1 km	15 min	73 s
Flood map module		25 m	1 km	15 min	7 s
Impact assessment module	Population	25 m	1 km	15 min	10 s
	Critical infrastructures	25 m	1 km		
	Regional summary	n/a	NUTS 2 or 3		

section 2.1) and the national flood maps produced in the framework of the EU Floods Directive (European Commission, 2007). Following the regional approach of Ritter et al. (2020), this connection is established based on the minimum distance between the ERICHA drainage network cells and the inundated areas in the flood maps: Each floodplain section is assigned to the nearest ERICHA drainage network cell.

When operating at European scale, however, a few adjustments are necessary: The flood maps of the Member States were created using a variety of hydraulic modelling approaches (for an overview, see European Commission, 2015a). Not only the modelling approaches but also the specifications of the flood maps vary considerably across the EU (Alfieri et al., 2014; Dottori et al., 2021). For instance, there are no common guidelines regarding the return periods modelled by the Member States (De Moel et al., 2009; European Commission, 2015b; Priest et al., 2016). Even within countries, the chosen return periods can vary between regions (e.g. in Germany, where the federal states are responsible for creating the maps). To achieve a certain homogeneity across Europe, we have used in each location the flood map of the highest available return period (e.g. in Spain the map of T = 500 years; see Fig. 2b) as a proxy of the maximum possible flood extent, hereafter referred to as "the floodplain". To make use of the high-resolution information contained in the floodplain maps, we have chosen to preprocess the maps as follows:

First, the floodplain geometries have been rasterised to a grid of 25 m resolution, as also done by the regional high-resolution method of Ritter et al. (2020). This gridded high-resolution floodplain is used for preprocessing the exposure layers (details follow in section 2.3). Then, the gridded high-resolution floodplain has been upscaled to 1 km resolution. The 1-km cells containing floodplains are hereafter referred to as "floodplain cells" (see Fig. 2b) and are used in the real-time calculations. To establish the link between the floodplains and the ERICHA drainage network, each floodplain cell has been assigned (by minimum distance) to the nearest ERICHA drainage network cell(s). Fig. 2a–c illustrates how the flood map module uses this assignment in real-time operation: If the ERICHA system identifies a FF hazard in a drainage network cell (Fig. 2a), the hazard level is automatically transmitted to all the floodplain cells assigned to this drainage network cell. The result is a map showing hazard levels in the potentially affected floodplains (Fig. 2c).

2.3. Impact assessment module

The aim of the impact assessment module is to estimate the socio-economic FF impacts in real time. For this purpose, it combines the hazard levels in the floodplains (generated by the flood map module; section 2.2) with information on socio-economic exposure. In ReAFFINE, impacts are estimated in terms of the potentially affected population (section 2.3.1) and critical infrastructures (section 2.3.2). To provide the end-user with a situational overview of the areas with the highest potential impacts, ReAFFINE also summarises the simulation results at the level of administrative regions (section 2.3.3).

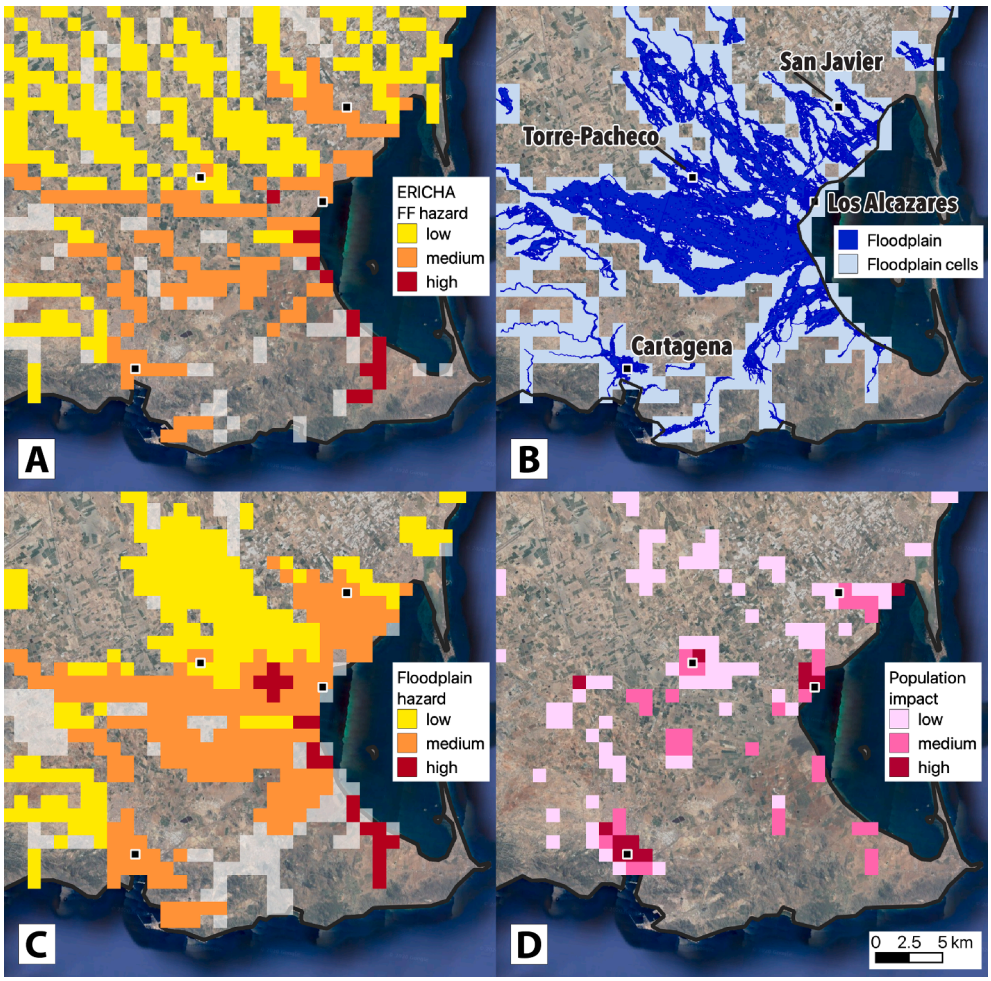

Fig. 2. Examples of the ReAFFINE inputs and outputs (13 September 2019 05:00 UTC) in the area around Los Alcazares (Southeast Spain; see the dashed box in Fig. 4). a) ERICHA FF hazard in the drainage network, b) Spanish flood map (T = 500 years) and corresponding floodplain cells employed by the flood map module, c) Floodplain hazard simulated by the flood map module, and d) Population impact simulated by the impact assessment module.

2.3.1. Impact on population

This component of the impact assessment module estimates in real time the impact on the population by counting the population potentially exposed to the hazard levels in the floodplain (generated by the flood map module; section 2.2). As a base for this step, we have used the population density map of Freire et al. (2016), covering all of Europe in 100 m resolution. For the application in ReAFFINE, the original dataset has been preprocessed offline as follows:

First, the resolution of the dataset has been increased to 25 m using nearest-neighbour interpolation. Then, population density values outside the floodplains have been removed, using the gridded high-resolution floodplain map described in section 2.2. Finally, the 25 m cells have been upscaled to 1 km resolution to match the grid of the floodplain cells. This process of downscaling-cropping-upscaling allows to determine offline in high resolution the population potentially exposed to flooding in each floodplain cell, before aggregating this information to a resolution that is suitable for real-time simulations at European scale.

In real-time operation, ReAFFINE uses the preprocessed population exposure map to estimate the impact on the population. In addition to counting the population potentially exposed to FF hazard (more detail follows in section 2.3.3), the potential impact the on population is also mapped in real time. This is done by means of an impact matrix (Fig. 3) that combines in each 1 km cell the three floodplain hazard levels (Fig. 2c) with three population exposure classes: low (1–99 people / km^2), medium (100–999 people / km^2), and high (1 000 and more people / km^2); these thresholds are arbitrary and have been manually adjusted. The result of applying the impact matrix is a map showing in each 1 km cell the population impact in terms of three qualitative impact levels (low-medium-high; see Fig. 2d for an example).

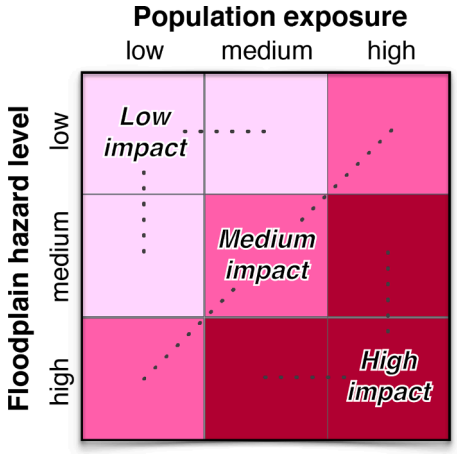

Fig. 3. Impact matrix that qualitatively estimates the FF impact on population by combining in each floodplain cell the hazard level with the population exposure class.

2.3.2. Impact on critical infrastructures (CIs)

ReAFFINE estimates the FF impact on critical infrastructures (CIs) by counting in real time the CIs potentially exposed to the hazard levels in the floodplains. This is done based on a CI dataset extracted from OpenStreetMaps in the frame of the project "Global Exposure Data for Risk Assessment" (Giovando et al., 2020). In ReAFFINE, we have included education facilities (EF), health facilities (HF), and mass-gathering sites (MG), and it is planned to add other CI types that will become available soon with European coverage (e.g. roads and railways).

Each of the three CI layers has been preprocessed offline in high resolution: First, only the CIs inside the gridded high-resolution floodplains (see section 2.2) have been kept in the inventory to maintain only the CIs potentially exposed to flooding. Then, the numbers and types of CIs have been counted in each 1-km floodplain cell. In real-time operation, ReAFFINE retrieves the numbers and types of CIs in all floodplain cells where the flood map module (section 2.2) identified a floodplain hazard. The result is a list of the exposed CIs in each floodplain cell.

2.3.3. Regional impact summary

When monitoring the real-time impact estimates at large spatial scales, it can be difficult and time-consuming for the end-user to identify the areas with the highest potential impacts. To assist in this task, ReAFFINE summarises the simulated impacts (described in sections 2.3.1 and 2.3.2) for each time step at the level of administrative regions. To ensure a homogeneous region size across country borders, we have used the combination of NUTS 2 (e.g. in Germany) and NUTS 3 regions (e.g. in Spain) proposed by Dottori et al. (2017) for the impact aggregation. As illustrated in Table 2, ReAFFINE summarises for each region the following information:

i) the overall exposed population (i.e. the sum of people potentially affected by any of the three floodplain hazard levels),
ii) totals of exposed population and CIs, listed separately for each of the three floodplain hazard levels, and
iii) the regional impact level, which is assigned as the maximum floodplain hazard level affecting population or CIs.

In the impact summary (Table 2), the regions are sorted in descending order of overall exposed population amounts (point i of the above list) to direct the attention of the end-user towards the regions with the highest numbers of potentially affected people. To complement the impact summary, the regional impacts are also mapped (Fig. 4): The regions are coloured according to the maximum floodplain hazard level affecting the population or CIs (point iii of the above list). This is done to also highlight high hazard levels that affect only small amounts of population or CIs since the localised nature of FFs can pose a potentially fatal risk to a very limited area.

3. Results

We have applied ReAFFINE to two FF events of recent years that caused numerous fatalities and billions of Euros in economic losses: The Elvira storm in Central Europe in spring 2016 and a cut-off low (DANA) in Spain in autumn 2019. In this section, we demonstrate the performance of ReAFFINE for these two events in Germany and Spain, using the national flood maps of these two countries (BfG, 2020; IGN, 2020).

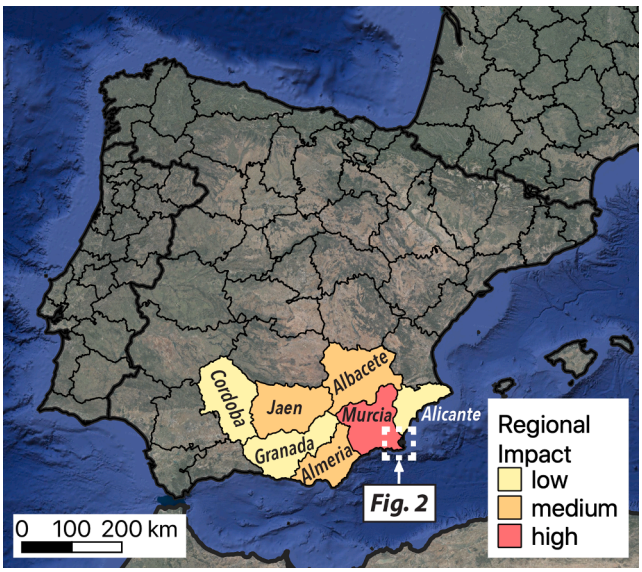

Fig. 4. Example of the regional impact summary map at a specific time step during a FF event (13 September 2019 05:00 UTC; corresponding to the situation in Table 2 and Fig. 2).

The simulated FF impacts presented in this section have been generated by running ReAFFINE on rainfall observations (rather than forecasts). This has been done to minimise external uncertainties and focus on the method's capabilities and limitations of translating FF hazards into impacts.

To evaluate the performance of the method, the simulation results have been compared with the impacts reported by civil protection authorities, insurance companies, news agencies, and social media. Such flood impact observations are inherently subject to high uncertainties (e.g. Brouwer et al., 2017; Ritter et al., 2020) and they typically contain impacts not only from FFs but also from other flood types that ReAFFINE is not designed to detect. This impedes a fully fair quantitative comparison between the simulated and the reported impacts, and therefore the results in this study have been evaluated mostly from a qualitative point of view.

While inspecting the ReAFFINE outputs in the following subsections, it is necessary to keep in mind that the primary objective of the method is to estimate FF impacts from a large-scale perspective (across regions or countries). The detection of more accurate impact locations and magnitudes is the aim of the regional high-resolution approaches mentioned in section 1.

Table 2
Example of the quantitative impact summary at a specific time step during a FF event (13 September 2019 05:00 UTC; corresponding to the situation in Fig. 2 and Fig. 4). The CIs are abbreviated as education facilities (EF), health facilities (HF), and mass-gathering sites (MG).

Region (country)	Population exposed	Population exposed to			CIs exposed to			Regional impact
		High hazard	Med. hazard	Low hazard	High hazard	Med. hazard	Low hazard	
Murcia (ES)	55 862	74	46 385	9 403		6 EF, 6 HF, 7 MG	2 HF	high
Almeria (ES)	4 916	0	1 461	3 455				med.
Jaen (ES)	258	0	258	0				med.
Albacete (ES)	126	0	20	106				med.
Cordoba (ES)	361	0	0	361				low
Alicante (ES)	167	0	0	167				low
Granada (ES)	97	0	0	97				low

3.1. Event 1: The low-pressure system Elvira in Central Europe in 2016

From the end of May to early June 2016, the stationary low-pressure system Elvira induced large rainfall amounts across Central Europe. The most significant impacts occurred in Germany and France. While in France mostly large rivers overflowed their banks (e.g. the Seine in Paris), the situation in Germany was characterised by numerous slow-moving and fast-evolving convective cells that caused severe FFs and pluvial floods across the country (Piper et al., 2016). According to Munich Re (2017), the overall economic damages in Germany amounted to 2.6 billion Euros and a total of ten people lost their lives due to the floods. The most devastating FFs occurred on 29 May in the village of Braunsbach in the Stuttgart region (Bronstert et al., 2018; Bronstert et al., 2017) and on 01 June in Simbach am Inn (Niederbayern) where five people died (LfU, 2016; TUM, 2017).

Fig. 5 shows the accumulated precipitation for the most intense period of the Elvira storm in Germany (29 May – 03 June 2016). It can be seen that the real-time adjusted OPERA radar rainfall (using the method of Park et al., 2019) corresponds reasonably well to the rainfall accumulations measured by the SYNOP raingauges (WMO, 2016).

The real-time adjusted radar rainfall maps (2 km and 15 min resolution) have been used as input for ReAFFINE. Over the entire duration of the event, this resulted in the simulated impacts summarised in Table 3 and Fig. 6a. ReAFFINE detected impacts in 35 of the 38 German NUTS 2 regions (i.e. all except Berlin, Hamburg, and Schleswig-Holstein). The regions with the most severe simulated impacts correspond reasonably well to those of the reported impacts (Table 3 and Fig. 6): In the 20 regions with the highest simulated impacts, impacts were also reported in reality, either by the European Severe Weather Database (ESWD; www.eswd.eu), or through the Tweets collected by Global Flood Monitor (www.globalfloodmonitor.org; de Bruijn et al., 2018, 2019). Among the overall 38 German regions, we have identified 31 with both simulated and reported impacts, 4 with simulated but no reported impacts, and 2 with reported but no simulated impacts.

In some regions, the magnitudes of the simulated impacts do not correspond very well to the magnitude of the reported impacts. For instance, the amounts of exposed population seem to be overestimated in the regions of Dusseldorf (609 704), Koln (186 201), and Darmstadt (133 399; Table 3). This is due to the Rhine River passing through these regions with an extremely wide floodplain (up to 25 km in the Dusseldorf region): A significant share of the Rhine's floodplain is assigned to several small tributaries – rather than to the Rhine itself – since ReAFFINE's flood map module operates based on the minimum distance between floodplains and assigned streams (as explained in section 2.2). In some of these tributaries, the ERICHA system estimated low to medium FF hazard, resulting in widespread floodplain hazard levels and thus overestimated impacts in these three regions.

With an exposed population of almost 194 000, the region of Stuttgart has been correctly identified as one of the most severely impacted by the storm (Table 3). However, ReAFFINE did not detect any population exposed to high hazard in this region. This does not seem to be in line with the three fatalities (Table 3) and the FF in the village of Braunsbach with a return period "clearly above 100 years" (Bronstert et al., 2018). The reason for the underestimation of the impact magnitude in the Stuttgart region is that the radar did not fully capture the extreme rainfall intensities in the small convective cells: For instance, in the small catchment upstream of Braunsbach (6 km^2), the real-time adjusted radar (Fig. 5a) estimated rainfall accumulations of 46–54 mm in 24 h (29 September 08:00 UTC – 30 September 08:00 UTC), whereas Bronstert et al. (2018) reconstructed a value of 135–153 mm for an almost identical time period. Due to the underestimated rainfall intensities, the ERICHA FF hazard did not exceed the medium level in Braunsbach, and thus ReAFFINE did not detect any population exposed to a high hazard.

In three locations in Germany, ReAFFINE identified populations exposed to high hazard levels (Table 3 and Fig. 6a): In the town of Ilmenau (Thuringen) that suffered severe flash floods (Deutsche Welle, 2016), ReAFFINE estimated 1 061 people exposed to high hazard (Table 3). Furthermore, 348 people exposed to high hazard were identified in the village of Obernzenn (Mittelfranken; Table 3) that also experienced severe flooding (Nürnberger Presse, 2016). Lastly, also in Niederbayern, which was the most affected region with seven fatalities and economic losses of around 1.25 billion Euros (LfU, 2016), ReAFFINE identified population exposed to high hazard (Table 3).

To add more quantitative components to the evaluation, we have also analysed the results at the level of the 401 districts in Germany (NUTS 3 regions; Table 4). For reference, we have considered that impacts occurred in those districts with either Tweets or ESWD reports. In 29.4 % of the German districts, impacts were both simulated and reported, whereas false alarms affected 48.6 % of the districts; i.e. impacts were simulated (in many cases with weak signals) but no Tweets or ESWD reports were issued in those districts (Table 4). Finally, impacts were missed in 4 % of the districts. These results translate to a high probability of detection of POD = 0.89 and a critical success index of CSI

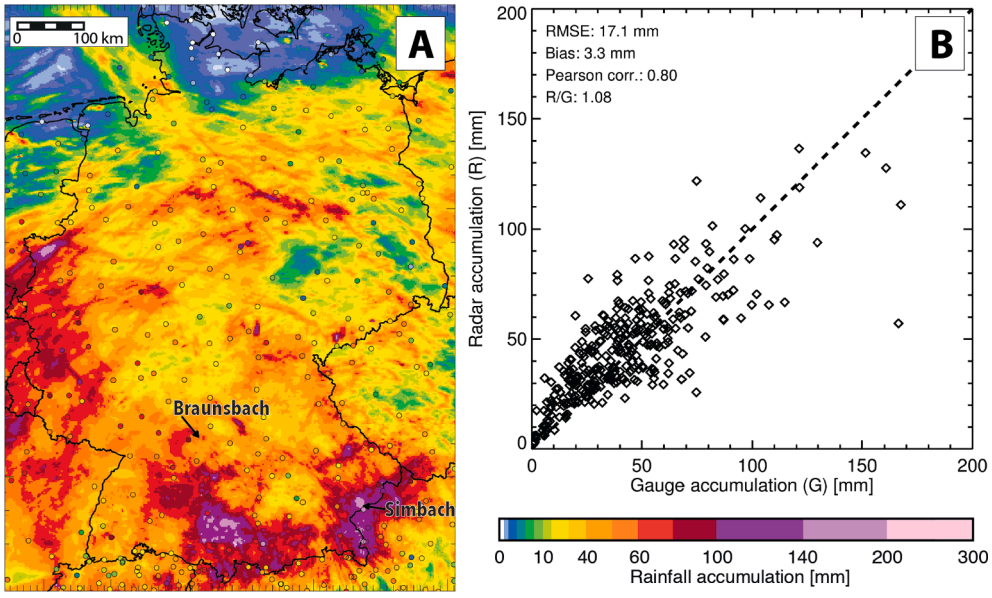

Fig. 5. Real-time adjusted OPERA radar rainfall (R) and SYNOP raingauge accumulations (G) in Germany for the most severe period of the Elvira storm (29 May – 03 June 2016): a) Map of precipitation amounts (raingauges are shown as circles), and b) Comparison of the real-time adjusted OPERA radar rainfall estimates to the accumulations measured by the collocated SYNOP raingauges. The quality scores in panel b represent the root-mean-square error (RMSE), the mean bias, the Pearson correlation, and the ratio of overall radar and raingauge accumulations (R/G).

Table 3
Simulated and reported impacts of the Elvira event (29 May – 03 June 2016; corresponding to Fig. 6). In total, ReAFFINE identified impacts in 35 regions; the 20 regions with the highest amounts of exposed population are listed here.

REGION	SIMULATED IMPACTS							REPORTED IMPACTS		
	Population exposed	Population exposed to			CIs exposed to			Regional impact			
		High hazard	Med. hazard	Low hazard	High hazard	Med. hazard	Low hazard		#Fatalities	#ESWD reports	#Tweets
Dusseldorf	609 704	0	24 423	585 281		4 EF, 4 HF, 7 MG	204 EF, 74 HF, 101 MG	med.		19	117
Stuttgart	193 692	0	75 298	118 394		40 EF, 18 HF, 15 MG	138 EF, 47 HF, 23 MG	med.	3	8	430
Koln	186 201	0	20 609	165 592		3 EF, 6 HF, 5 MG	38 EF, 21 HF, 20 MG	med.		2	35
Darmstadt	133 399	0	0	133 399			44 EF, 33 HF, 25 MG	low		18	16
Oberbayern	118 702	0	17 994	100 708		1 EF, 4 HF, 2 MG	33 EF, 29 HF, 18 MG	med.			33
Karlsruhe	102 844	0	11 718	91 126		8 HF, 7 MG	78 EF, 25 HF, 15 MG	med.		9	68
Schwaben	85 818	0	21 847	63 971		6 EF, 1 HF, 4 MG	71 EF, 14 HF, 18 MG	med.		23	33
Tubingen	84 604	0	22 681	61 923		18 EF, 5 HF, 7 MG	120 EF, 23 HF, 12 MG	med.		2	10
Munster	84 245	0	13 459	70 786		17 EF, 3 HF, 1 MG	23 EF, 15 HF, 26 MG	med.		1	17
Niederbayern	76 972	67	8 751	68 154		9 EF, 6 MG	36 EF, 24 HF, 14 MG	high	7	26	1 650
Sachsen-Anhalt	64 941	0	4 221	60 720		2 EF	10 EF, 10 HF, 15 MG	med.		5	3
Thuringen	52 930	1 061	2 287	49 582	5 EF, 1 HF	4 EF, 1 HF	53 EF, 11 HF, 7 MG	high		4	18
Arnsberg	32 547	0	0	32 547			23 EF, 8 HF, 4 MG	low			2
Dresden	27 625	0	10	27 615			11 EF, 5 HF, 2 MG	med.		16	11
Brandenburg	25 994	0	98	25 896			3 EF, 9 HF, 5 MG	med.		9	
Rheinhessen-Pfalz	25 014	0	0	25 014			26 EF, 4 HF, 7 MG	low		2	7
Koblenz	23 434	0	0	23 434			35 EF, 12 HF, 1 MG	low		23	43
Mittelfranken	23 049	348	4 798	17 903		1 EF, 3 HF	12 EF, 14 HF, 1 MG	high		10	24
Unterfranken	22 663	0	718	21 945			35 EF, 10 HF, 8 MG	med.		10	23
Freiburg	19 868	0	82	19 786			3 EF, 2 HF, 14 MG	med.			3

= 0.36. The relatively low CSI is the consequence of the high number of false alarms, which are partly due to the inherent incompleteness of impact observations, especially in areas that experienced only minor impacts (for an impression of the high uncertainties in the impact datasets, see the discrepancies between the ESWD reports and the Tweets in Figs. 6b and 7).

To evaluate the simulation results at even smaller spatial scales, we take a closer look at the most severely affected region of Niederbayern. As a reference for the simulated impacts, we have used the impact observations from Twitter and the European Severe Weather Database (previously shown in Fig. 6b), and additionally the regional flood observations from the Bavarian Environment Agency (LfU, 2016). The ERICHA system simulated widespread FF hazard in the drainage network across Niederbayern (Fig. 7a). The FF hazard signals appear in most of the locations with impact evidences from ESWD, LfU, or Tweets. On the other hand, also large areas without reported impacts show FF hazard (e.g. the rural north-eastern part of the region). In the town of Simbach am Inn, which suffered unprecedented flooding with five fatalities (LfU, 2016; TUM, 2017), the ERICHA FF hazard in the Simbach stream (30 km^2) did not exceed the medium level (Fig. 7a). The underestimation of the hazard in this location is due to a breach of a road embankment upstream of the town (LfU, 2016; TUM, 2017), which significantly increased the real flood magnitude in Simbach am Inn.

Based on the ERICHA FF hazard in the drainage network (Fig. 7a), the flood map module (section 2.2) estimated the hazard levels in the floodplains shown in Fig. 7b. Floodplain hazard signals are present in many of the reported impact locations, especially in the most severely affected areas such as Simbach am Inn (Fig. 7b). Furthermore, widespread ERICHA FF hazard signals in areas where no significant impacts occurred (e.g. in the North-east of the region; Fig. 7a) did not transform into floodplain hazard due to the lack of flood maps in these rural areas (Fig. 7b). On the other hand, also in some locations with reported impacts, the flood map module did not transform the ERICHA FF hazard into floodplain hazard. This can occur for two reasons: In some locations, the responsible authorities did not create flood maps due to the low (however existing) socio-economic exposure of the areas near the streams; see for instance the disappearance of the high hazard level in the small stream (28 km^2) near the village of Rattenberg in Fig. 7. In other locations (e.g. in Herrngiersdorf; Fig. 7), the reported impacts were not caused by FFs, but by surface runoff outside the floodplains (pluvial flooding; LfU, 2016).

To summarise the results of the Elvira storm: the impact estimates from a large-scale perspective corresponded relatively well to the observed regional impacts (Fig. 6). At sub-regional scale, the underlying uncertainty sources of the method became more apparent (e.g. the accuracy of the rainfall estimates or the coverage of the flood maps).

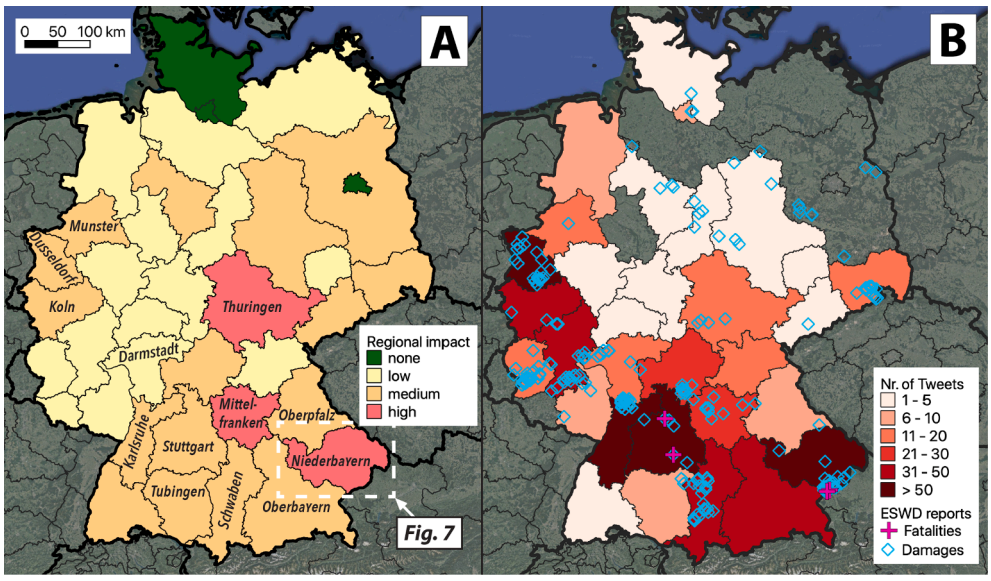

Fig. 6. a) Simulated regional impact summary of the Elvira event (29 May – 03 June 2016). b) Reported impacts: Number of flood-related Tweets per region (www.globalfloodmonitor.org; de Bruijn et al., 2018, 2019) and the locations of fatalities and damages reported by the European Severe Weather Database (ESWD; www.eswd.eu). Panels a and b correspond to the quantitative impact information in Table 3.

Table 4
Contingency table of simulated and observed impacts in the 401 German districts (NUTS 3 regions). "Impacts simulated" refers to the districts in which ReAFFINE identified population or CIs exposed to hazard levels. "Impacts observed" refers to the districts with Tweets or ESWD reports. The critical success index calculated from the listed numbers is CSI = 0.36.

		Impacts observed		
		YES	NO	Σ
Impacts simulated	**YES**	118	195	313
	NO	15	78	93
	Σ	133	273	401

Nevertheless, ReAFFINE succeeded to detect the regions of the most severe impacts (e.g. Niederbayern). Although the simulation results presented in this section have been aggregated over the full event duration, it should be noted that the timing of the simulated impacts in the most affected locations approximately coincided with the onsets of the floods. For instance, the medium hazard levels around Simbach am Inn appeared about 1 h before the first flooding in the town was reported (LfU, 2016).

3.2. Event 2: The DANA event of 2019 in Spain

In September 2019, a cut-off low – in Spain commonly known as DANA (Depresión Aislada en Niveles Altos; Martín León, 2003) – promoted the development of long-lasting convective systems that affected large parts of the country. Along the south-eastern Mediterranean Coast, rainfall accumulations of up to 461 mm in 24 h caused numerous FFs and a severe river flood in the downstream part of the Segura catchment (see e.g. Biener Camacho and Prieto Cerdán, 2019; ERCCa, 2019; García et al., 2020). Seven people lost their lives, over 6 000 were evacuated (DGPCE, 2019), and the overall economic losses were estimated to exceed 2.2 billion Euros (AON, 2019).

In contrast to the Elvira storm of spring 2016 (section 3.1), the accuracy of the real-time adjusted OPERA radar rainfall for the DANA event was relatively low (Fig. 8a and b). The radar located in Murcia had a malfunction during an important period of the event, resulting in a significant underestimation of the rainfall amounts. To mitigate this underestimation for the analysis of this event, we have (a posteriori) applied the radar-raingauge-blending method of Velasco-Forero et al. (2009; also described by Cassiraga et al., 2020), using the hourly observations of the raingauge network of the Spanish State Meteorological Agency. The resulting improved rainfall accumulations are shown in Fig. 8c and d.

Using the blended rainfall maps as input, ReAFFINE identified impacts in 14 of the 48 Spanish NUTS 3 regions in the domain. The regions with the highest simulated impacts (Fig. 9a) correspond very well to those reported by the Spanish Insurance Compensation Consortium (CCS, 2020) and the Spanish Directorate-General for Civil Protection and Emergencies (DGPCE, 2019; Fig. 9b). This is confirmed by the quantitative comparison of simulated and reported impacts (Table 5): ReAFFINE correctly identified Murcia and Alicante as the most severely affected regions. In the region of Malaga, the relatively high simulated impacts are the result of a local rainfall overestimation caused by a systematic interference of the signal of the Almeria radar (visible in the accumulations in Fig. 8c and d).

Of the overall 20 regions with insured losses greater than 10 thousand Euros (Table 6), ReAFFINE identified impacts in 14, which corresponds to a relatively high probability of detection of POD = 0.70. In combination with 0 false alarms, this resulted in a high critical success index of CSI = 0.70 (Table 6).

Fig. 10 shows the part of Spain that was most severely affected by the DANA storm. The ERICHA system detected significant FF hazard in almost all of the impact locations documented by the Spanish Civil Protection, the media, or the Twitter crowdsourcing (Fig. 10a). Moreover, the red hazard levels appear mostly in the areas where the density of reported impacts is highest.

In the great majority of the locations where the Civil Protection carried out rescues or evacuations, the flood map module expanded the hazard signals from the ERICHA system (Fig. 10a) into the floodplains (Fig. 10b). Furthermore, in many rural areas where no impacts occurred, hazard signals did not transform into floodplain hazard due to the lack of flood maps (e.g. in the North-east of the Alicante region). However, also in a few locations with reported impacts, FF hazard levels were not translated into floodplain hazard: For instance near the border between Alicante and Albacete, where two persons died on a flooded country road, the medium hazard level disappeared because no flood maps are available for the small rural stream (31 km^2; Fig. 10).

The impact assessment module combined the floodplain hazard

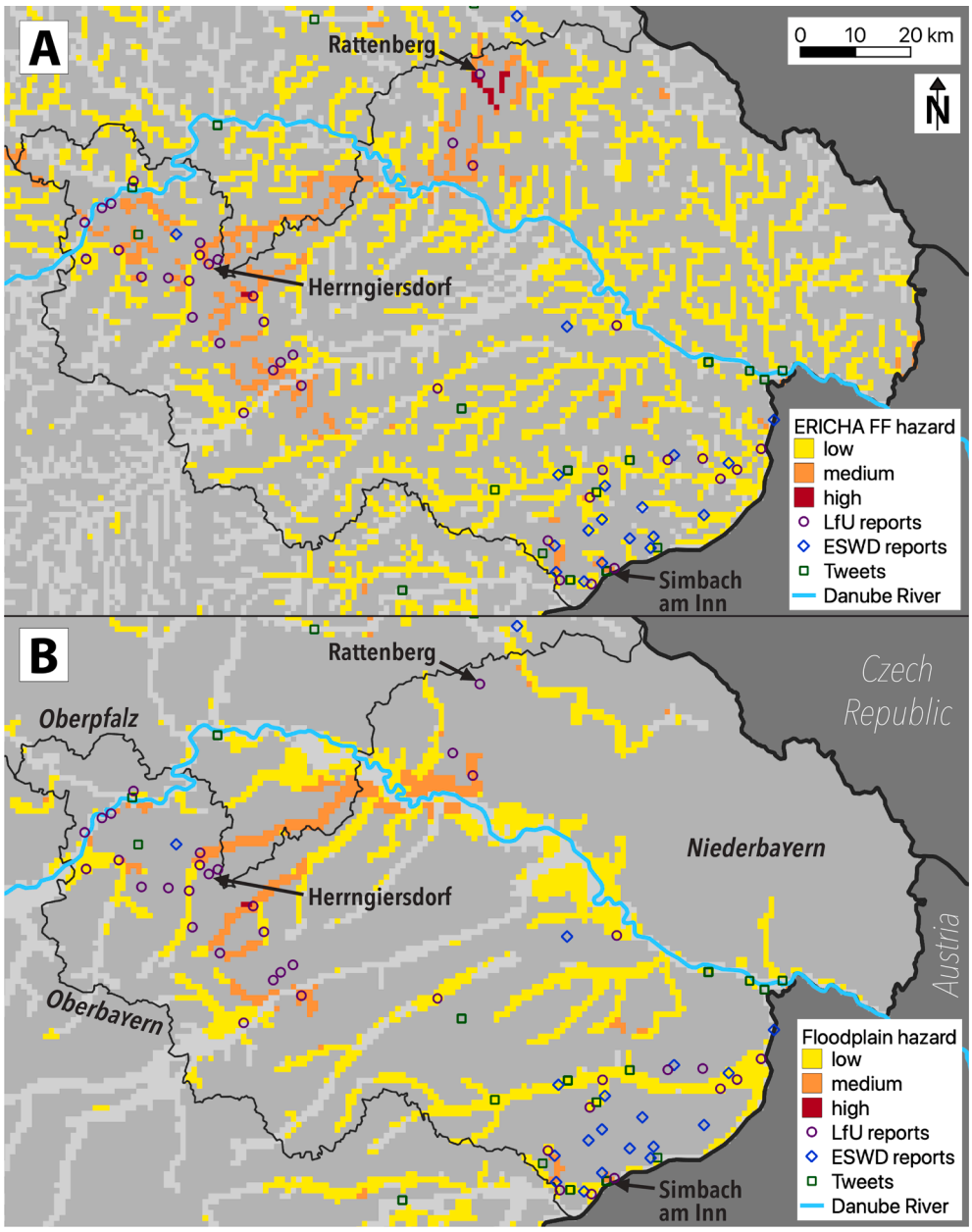

Fig. 7. The region of Niederbayern (the dashed box in Fig. 6a indicates the shown area): a) maximum FF hazard estimated by the ERICHA system, and b) maximum floodplain hazard estimated by the flood map module (29 May – 03 June 2016). In the streams in and around Simbach, a total of 15 ESWD reports were recorded; some have been removed in this figure for the sake of clarity.

(Fig. 10b) with the population exposure, resulting in the population impact levels shown in Fig. 11. The locations with high population impact coincide very well with the areas where the Spanish Civil Protection reported the most important FF impacts (DGPCE, 2019): in the severely affected towns of Ontinyent (upstream catchment area 160 km^2), Mogente (862 km^2), and Almansa (365 km^2) in the North of Fig. 11, as well as in Los Alcazares (101 km^2) and Torre-Pacheco (15 km^2) in the South. Along the Segura River, the impacts appear underestimated (judging from the density of flood observations). However, the impact processes in this area were strongly dominated by the exceptional fluvial flooding in the Segura River (affecting more than 5 000 ha of the floodplain; ERCCb, 2019). ReAFFINE is not designed to detect the fluvial flood component originating from the Segura River since the ERICHA system assesses the FF hazard only in the catchments smaller than 2 000 km^2 (whereas the drainage area of the Segura at the most severely affected location is about 15 000 km^2).

In summary, the performance of ReAFFINE for this DANA event is highly satisfactory. The regional impact estimates (Table 5 and Fig. 9) correlate exceptionally well with the reported impacts. Also at sub-regional scale, ReAFFINE accurately identified the areas where the most severe impacts were observed (Fig. 11). In addition, also the timing of the signals corresponded well with the flood occurrences (e.g. the time of the simulated impacts in Fig. 2d matched the approximate peak times of the floods in Los Alcazares and Torre-Pacheco). However, for the simulation of this event, the uncertainty in the rainfall inputs has been minimised (a posteriori). In real-time operation, impact estimates with lower accuracies should be expected due to the quality of the rainfall inputs.

4. Conclusions

This study introduces a novel method, named ReAFFINE, for

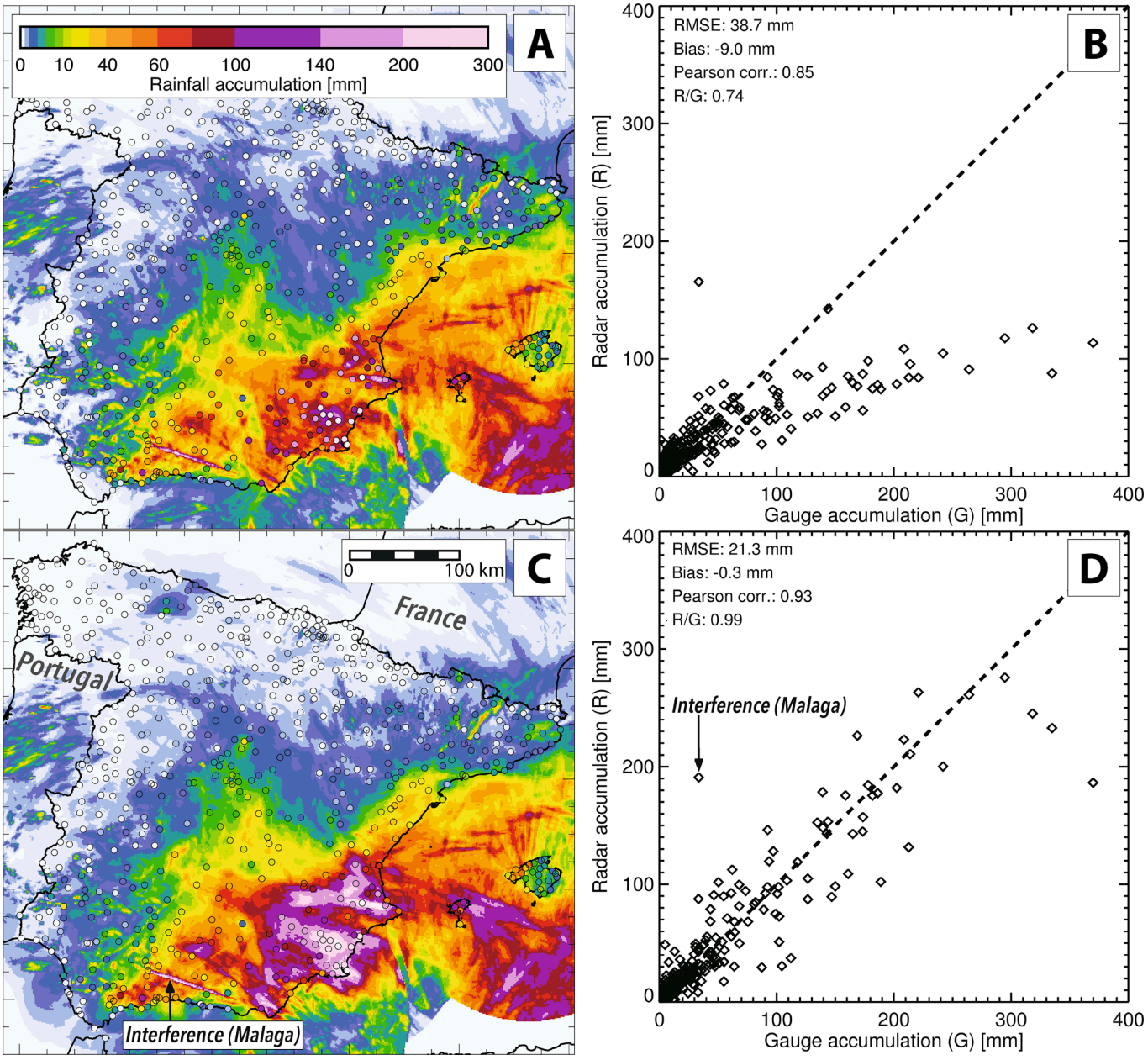

Fig. 8. Total rainfall accumulations in Spain (11–14 September 2019) from the real-time adjusted OPERA radar (a and b) and the radar-raingauge-blending (c). d) Performance of the radar-raingauge-blending using "leave-one-out" cross validation. The raingauge network of the Spanish State Meteorological Agency (AEMET) is illustrated by the circles in panels a and c. The quality scores in panels b and d represent the root-mean-square error (RMSE), the mean bias, the Pearson correlation, and the ratio of overall radar and raingauge accumulations (R/G).

assessing flash flood impacts in real time at pan-European scale. Until now, real-time flash flood impact assessments were limited to local or regional applications (e.g. Le Bihan et al., 2017; Calianno et al., 2013; Ritter et al., 2020; Silvestro et al., 2019) due to the high computational cost of these high-resolution approaches. ReAFFINE addresses this challenge by operating in real time at lower resolution (1 km), while the required high-resolution information (25 m) is incorporated through offline preprocessing. The method is designed to be integrated into a pan-European flash flood early warning system (EWS) to provide operational decision support for emergency services and other end-users operating over large spatial domains (e.g. national or European civil protection mechanisms or transboundary catchment authorities).

The method consists of three main elements: First, a hazard module (the ERICHA system; Corral et al., 2019; Park et al., 2017; Park et al., 2019) transforms rainfall inputs into estimates of the flash flood hazard over a gridded drainage network covering all of Europe. Secondly, a flood map module uses the national flood maps created through the EU Floods Directive (European Commission, 2007) to expand the flash flood hazard into the floodplains. Lastly, an impact assessment module combines the estimated hazard in the floodplains with socio-economic exposure information to identify the potentially affected population and critical infrastructures. The structure of the method allows for the integration of additional exposure and vulnerability layers. For instance, the dynamic population density maps from the ENACT project (Batista e Silva et al., 2017) or the HARCI-EU critical infrastructure grids (Batista e Silva et al., 2019) could be included to further enhance the impact estimation.

ReAFFINE has been tested for two severe flash flood events affecting Europe in recent years. The capability of the method to identify impacts over large spatial scales has been demonstrated; the simulation results

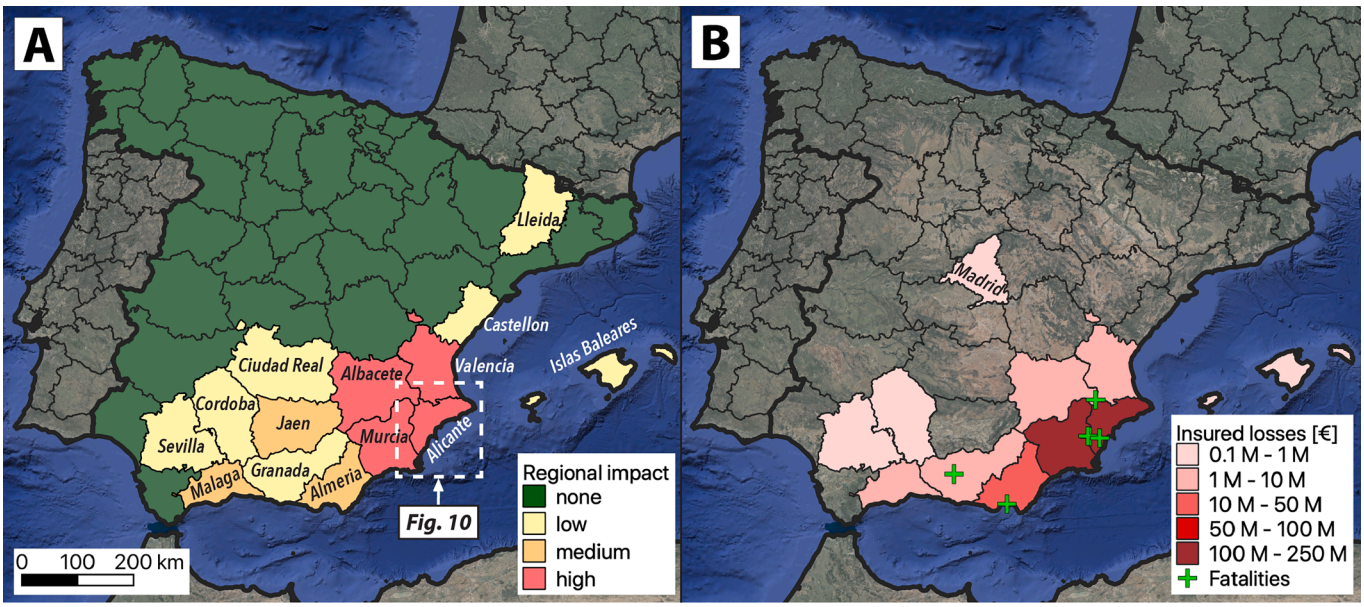

Fig. 9. a) Regional summary of simulated impacts for the DANA storm (11–14 September 2019). b) Reported impacts from flood insurance data (CCS, 2020) and the Spanish Civil Protection (DGPCE, 2019). The quantitative impacts corresponding to this figure are listed in Table 5.

Table 5
Simulated and reported impacts for the DANA event (11–14 September 2019; corresponding to Fig. 9).

REGION	SIMULATED IMPACTS								REPORTED IMPACTS		
	Population exposed	Population exposed to			CIs exposed to			Regional impact			
		High hazard	Med. hazard	Low hazard	High hazard	Med. hazard	Low hazard		# Fatalities	# Tweets	Insured losses [M€]
Murcia	182 900	1 860	129 258	51 782	1 HF	6 EF, 21 HF, 17 MG	4 EF, 8 HF, 4 MG	high		753	203.76
Alicante	79 327	2 188	27 167	49 972		10 EF, 12 HF, 7 MG	2 EF, 15 HF, 6 MG	high	3	736	201.98
Malaga	28 721	0	5 795	22 926		2 MG	1 EF, 1 HF, 5 MG	med.		15	5.09
Valencia	25 429	1 443	19 357	4 629		2 EF, 4 HF, 2 MG	1 EF, 1 HF, 1 MG	high		199	9.69
Almeria	18 861	0	3 817	15 044			1 EF	med.	1	165	11.32
Islas Bal.	4 391	0	0	4 391				low		14	0.28
Albacete	4 071	2 555	490	1 026				high	2	89	2.44
Granada	611	0	0	611				low	1	7	1.91
Sevilla	594	0	0	594				low		8	0.13
Jaen	509	0	258	251				med.		3	0.05 (<0.1)
Cordoba	361	0	0	361				low		3	0.35
Lleida	3	0	0	3				low		0	0.01 (<0.1)
Castellon	3	0	0	3				low		4	0.03 (<0.1)
Ciudad Real	3	0	0	3				low		0	0.02 (<0.1)
Madrid	0	0	0	0				none		44	0.65

Table 6
Contingency table of the simulated and observed impacts in the 48 Spanish provinces in the domain (NUTS 3 regions). "Impacts simulated" refers to the provinces in which ReAFFINE identified population or CIs exposed to hazard levels. "Impacts observed" refers to the provinces with insured losses greater than 10 thousand Euros. The critical success index calculated from the listed numbers is CSI = 0.70.

		Impacts observed		
		YES	NO	Σ
Impacts simulated	**YES**	14	0	14
	NO	6	28	34
	Σ	20	28	48

generally corresponded well to the impacts reported by various validation sources. However, it has been found that a number of factors influence the performance of the method, some of them due to inaccuracies in the employed datasets (hereafter referred to as "uncertainties"), others due to assumptions and methodological choices made by the components of ReAFFINE (hereafter referred to as "limitations"):

- Rainfall inputs: The quality of the rainfall inputs is one of the most significant factors affecting the accuracy of the simulated flash flood impacts (confirming the findings of Ritter et al., 2020). Although being improved through the method of Park et al. (2019), the real-time OPERA radar rainfall remains subject to high uncertainties. These uncertainties can be mitigated by blending the radar rainfall

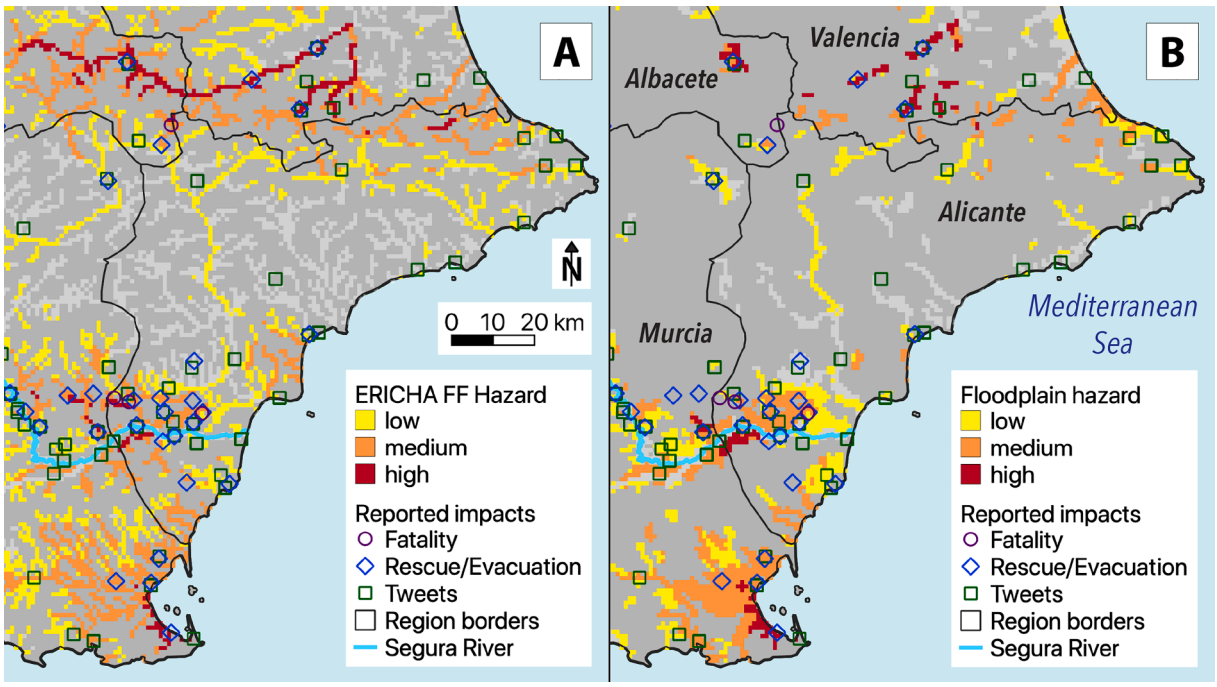

Fig. 10. The south-eastern regions of Spain (the dashed box in Fig. 9a indicates the shown area): a) maximum FF hazard estimated by the ERICHA system, and b) maximum floodplain hazard estimated by the flood map module (11–14 September 2019). The reported impact locations have been obtained from the Spanish Civil Protection (DGPCE, 2019), the news articles compiled in CRAHI (2019), and from the Tweets collected by Global Flood Monitor (www.globalfloodmonitor.org; de Bruijn et al., 2018, 2019).

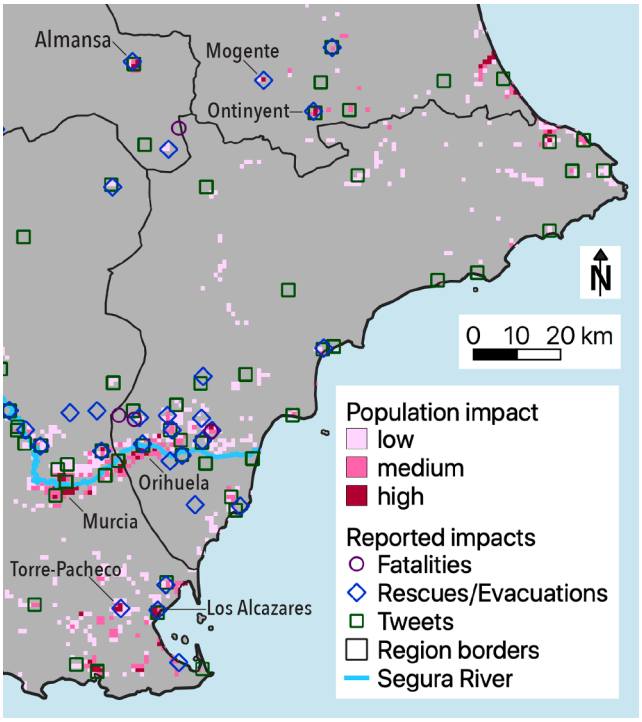

Fig. 11. Maximum population impact over the full event duration (corresponding to Fig. 10), simulated by the impact assessment module via the impact matrix (section 2.3.1).

with raingauge observations (as done for the second event; section 3.2). However, at European scale, this technique is not yet available in real time due to the hurdles described by Park et al. (2019).

In this study, rainfall observations have been used as input to minimise external uncertainties and focus on the translation of rainfall inputs into socio-economic impacts. For usage in operational conditions, it would be beneficial to employ also rainfall forecasts as inputs (e.g. from radar nowcasting) to increase the anticipation time of the warnings. To quantify the benefits of using rainfall forecasts, it would be important to carry out a sensitivity analysis of the influence of this additional uncertainty source on the accuracy of the warnings.

- ERICHA flash flood hazard estimation: Given a sufficiently high quality of the rainfall inputs, the ERICHA system appeared to provide reliable flash flood hazard estimates: Using the radar-raingauge-blending as rainfall input (as done in the second event; section 3.2), the areas with the highest simulated hazard levels corresponded well to the areas where the most severe flash floods occurred. In comparison, the hazard estimates in the first event (section 3.1) showed a lower accuracy, likely due to the higher uncertainty in the rainfall inputs (compare the quality scores of the rainfall inputs in Figs. 5b and 8d).
  The purely rainfall-based hazard estimation not accounting for potentially important factors such as pre-event soil moisture can result in underestimated or overestimated hazards in wet or dry catchments, respectively. In the two analysed extreme events, this limitation has not been apparent, but it is expected to have a larger influence during events of lower magnitudes (see e.g. Corral et al., 2019; Grillakis et al., 2016; Ritter et al., 2020).
- Flood map module: The added value of applying the national flood maps for a refined hazard estimation is twofold: Firstly, it expands the hazard signals into the floodplains and thus enhances the identification of potentially affected areas. Secondly, the hazard signals are condensed to the parts of the stream network where flood maps are available, which are – by definition – the areas where the national authorities identified significant flood risks (European Commission, 2007). The resulting hazard levels in the floodplains concentrate on the high-risk areas and are thus potentially easier to interpret for the end-user. However, in both analysed events, we have observed occasional gaps in the flood maps in streams that are

small but do represent a significant risk (similarly as found by Ritter et al., 2020). In such streams, the application of the flood maps can lead to the removal of the hazard signal and thus in an underestimation of the impacts.

Near rivers with large floodplains (e.g. the Rhine and the Danube in the first event; section 3.1), the application of the flood maps can cause an overestimation of impacts: ReAFFINE assigns significant parts of the large floodplains to small tributaries, resulting in simulated flash flood impacts where flood risks are mostly due to the large rivers. In the future, this limitation could be mitigated if the national authorities provide the flood extents separately for each stream (as already done e.g. in some basins in Spain; IGN, 2020), instead of merging the flooded areas from large rivers and their tributaries. A less effective but intermediate mitigation measure of this limitation could be to filter the simulation results of ReAFFINE by applying a mask of the large river floodplains (e.g. using the EFAS flood maps for rivers with catchment areas larger than 500 km^2; Dottori et al., 2021).

- Impact assessment module: Combining the hazard levels in the floodplains with socio-economic exposure information enabled a quantitative estimation of the potentially affected population and critical infrastructures for each region. The magnitudes of these regional impact estimates mostly corresponded to those reported by various validation sources. At sub-regional level, the distributed population impact levels (resulting from the application of the impact matrix) mostly succeeded to point out the towns that suffered the most important impacts. For instance in the second event (section 3.2), a high population impact was simulated for almost all of the towns where the Civil Protection carried out rescues or evacuations due to flash floods (DGPCE, 2019).

The presented results of the two flood events have illustrated some of the capabilities and limitations of the method. The results of the second event (section 3.2) have recently been compared to those obtained using a regional high-resolution method, and the results showed a high agreement (Ritter et al., 2021a). However, it would be important to test ReAFFINE also over a continuous time period (e.g. 1–2 years) and systematically evaluate the results (e.g. using contingency tables). A full evaluation would require testing the method in an operational setting and gathering feedback from the end-users regarding the usefulness of the method for operational decision-making.

As illustrated by both of the analysed events, flood impacts are often the result of a combination of different flood types: In the first event (section 3.1), pluvial floods exacerbated the impacts induced by the flash floods, while in the second event (section 3.2), a coinciding fluvial flood in the Segura River was responsible for a significant share of the losses. For these so-called compound events (e.g. Zscheischler et al., 2018; Zscheischler et al., 2020), the flood type-specific forecasting methods traditionally developed by the scientific community are unable to detect the overall impacts (Merz et al., 2020). The decision support for the end-users could be significantly improved by integrating different flood type-specific methods into an overall flood impact forecast. This idea has been explored in a separate study (Ritter et al., 2021b) that assessed the compound impacts of the second event (section 3.2), using a combination of two methods designed for flash floods (Ritter et al., 2020) and river floods (Dottori et al., 2017).

In a recently published comprehensive review on impact forecasting methods, Merz et al. (2020) concluded that "impact forecasting tends to be more context-specific than hazard forecasting. In some cases, first-order estimates providing order of magnitude statements might suffice to support rescue operations in the very aftermath of the disaster. In other cases, detailed and location-specific information about the expected impacts might be required to trigger specific emergency measures, such as evacuating a hospital". While the existing regional flash flood impact forecasting methods may serve as decision support for location-specific emergency measures (even up to the detail of site-specific warnings; see Landaverde et al., 2020), ReAFFINE is capable of providing order-of-magnitude estimates from a large-scale perspective. This represents a significant complement to the existing decision support, in particular for end-users operating at larger spatial scales.

ReAFFINE is ready for implementation in a pan-European EWS. In this study, the impact simulations in Germany and Spain have been analysed, but the prerequisites for applying the method are met throughout the EU: The ERICHA flash flood hazard system is already implemented in real time across Europe and the employed socio-economic exposure layers cover the entire continent. Including additional countries in ReAFFINE is relatively simple: Only the national flood maps are required for the preprocessing of the exposure layers (see section 2), and an increasing number of European countries share their flood maps on the INSPIRE platform (https://inspire.ec.europa.eu). Such initiatives for standardising and sharing data across borders pave the way towards future developments of forecasting solutions over large spatial scales. In the context of ReAFFINE, the harmonisation of historical rainfall records and commonly defined return periods for the creation of the national flood maps would allow for further enhancements of the method. For instance, it would enable fully quantitative real-time assessments of affected population, critical infrastructures, and economic losses across Europe.

CRediT authorship contribution statement

Josias Ritter: Conceptualization, Methodology, Software, Validation, Investigation, Visualization, Writing – original draft. **Marc Berenguer:** Conceptualization, Methodology, Supervision, Writing - review & editing. **Shinju Park:** Conceptualization, Resources, Data curation. **Daniel Sempere-Torres:** Conceptualization, Supervision, Resources, Project administration, Funding acquisition.

Declaration of Competing Interest

The authors declare that they have no known competing financial interests or personal relationships that could have appeared to influence the work reported in this paper.

Acknowledgements

The EU Horizon 2020 project ANYWHERE (H2020-DRS-1-2015-700099) financed the initial period of this work. The study was finalised in the framework of the TAMIR project (UCPM-874435-TAMIR). We would like to express our gratitude to OPERA, WMO and the Spanish State Meteorological Agency (AEMET) for the provision of meteorological data, and the Spanish National Geographic Institute (IGN) and the German Federal Institute of Hydrology (BfG) for access to the national flood maps. Furthermore, we would like to thank OpenStreetMaps, Milan Kalas, and the Joint Research Centre for providing the pan-European exposure datasets, and the European Severe Weather Database (ESWD), the Bavarian Environment Agency (LfU), the Spanish Insurance Compensation Consortium (CCS), the Spanish Directorate-General for Civil Protection and Emergencies (DGPCE), and Jens de Bruijn (Vrije Universiteit Amsterdam) from the Global Flood Monitor for meticulously reporting the impacts of the analysed flood events.

References

Alfieri, L., Berenguer, M., Knechtl, V., Liechti, K., Sempere-Torres, D., Zappa, M., 2019. Flash Flood Forecasting Based on Rainfall Thresholds. In: Handbook of Hydrometeorological Ensemble Forecasting. Springer Berlin Heidelberg, Berlin, Heidelberg, pp. 1223–1260. https://doi.org/10.1007/978-3-642-39925-1_49.

Alfieri, L., Salamon, P., Bianchi, A., Neal, J., Bates, P., Feyen, L., 2014. Advances in pan-European flood hazard mapping. Hydrol. Process. 28, 4067–4077. https://doi.org/10.1002/hyp.9947.

Alfieri, L., Salamon, P., Pappenberger, F., Wetterhall, F., Thielen, J., 2012. Operational early warning systems for water-related hazards in Europe. Environ. Sci. Policy 21, 35–49. https://doi.org/10.1016/j.envsci.2012.01.008.

Alfieri, L., Thielen, J., 2015. A European precipitation index for extreme rain-storm and flash flood early warning. Meteorol. Appl. 22, 3–13. https://doi.org/10.1002/met.1328.

AON, 2019. Global Catastrophe Recap - September 2019.

Barredo, J.I., 2007. Major flood disasters in Europe: 1950–2005. Nat. Hazards 42, 125–148. https://doi.org/10.1007/s11069-006-9065-2.

Batista e Silva, F., Forzieri, G., Marin Herrera, M.A., Bianchi, A., Lavalle, C., Feyen, L., 2019. HARCI-EU, a harmonized gridded dataset of critical infrastructures in Europe for large-scale risk assessments. Sci. Data 6, 1–11. 10.1038/s41597-019-0135-1.

Batista e Silva, F., Rosina, K., Schiavina, M., Marin Herrera, M.A., Freire, S., Craglia, M., Lavalle, C., 2017. Spatiotemporal mapping of population in Europe: The "ENACT" project in a nutshell, 57th European Regional Science Association (ERSA) Congress. pp. 1–17.

BfG, . Geoportal der Bundesanstalt für Gewässerkunde. accessed 10.21.20. https://geoportal.bafg.de/CSWView/od.xhtml. .

Biener Camacho, S., Prieto Cerdán, A., 2019. Inundaciones de septiembre de 2019 en la Vega Baja del Segura: causas y consecuencias. Canelobre 70.

Bronstert, A., Agarwal, A., Boessenkool, B., Crisologo, I., Fischer, M., Heistermann, M., Köhn-Reich, L., Andrés López-Tarazón, J., Moran, T., Ozturk, U., Reinhardt-Imjela, C., Wendi, D., 2018. Forensic hydro-meteorological analysis of an extreme flash flood: The event in Braunsbach. SW Germany. Sci. Total Environ. 630, 977–991. https://doi.org/10.1016/j.scitotenv.2018.02.241.

Bronstert, A., Agarwal, A., Boessenkool, B., Fischer, M., Heistermann, M., Köhn-Reich, L., Moran, T., Wendi, D., 2017. Die Sturzflut von Braunsbach am 29. Mai 2016 – Entstehung, Ablauf und Schäden eines „Jahrhundertereignisses". Teil 1: Meteorologische und hydrologische Analyse. Hydrol. und Wasserbewirtschaftung 61, 150–162. https://doi.org/10.5675/HyWa_2017,3_1.

Brouwer, T., Eilander, D., Van Loenen, A., Booij, M.J., Wijnberg, K.M., Verkade, J.S., Wagemaker, J., 2017. Probabilistic flood extent estimates from social media flood observations. Nat. Hazards Earth Syst. Sci. 17, 735–747. https://doi.org/10.5194/nhess-17-735-2017.

Calianno, M., Ruin, I., Gourley, J.J., 2013. Supplementing flash flood reports with impact classifications. J. Hydrol. 477, 1–16. https://doi.org/10.1016/j.jhydrol.2012.09.036.

Cassiraga, E., Gómez-Hernández, J.J., Berenguer, M., Sempere-Torres, D., Rodrigo-Ilarri, J., 2020. Spatiotemporal Precipitation Estimation from Rain Gauges and Meteorological Radar Using Geostatistics. Math. Geosci. https://doi.org/10.1007/s11004-020-09882-1.

CCS, 2020. Base de datos. Daños asegurados por inundación en España (2000-2019). Madrid.

Clark, R.A., Gourley, J.J., Flamig, Z.L., Hong, Y., Clark, E., 2014. CONUS-Wide Evaluation of National Weather Service Flash Flood Guidance Products. Weather Forecast. 29, 377–392. https://doi.org/10.1175/WAF-D-12-00124.1.

Corral, C., Berenguer, M., Sempere-Torres, D., Poletti, L., Silvestro, F., Rebora, N., 2019. Comparison of two early warning systems for regional flash flood hazard forecasting. J. Hydrol. 572, 603–619. https://doi.org/10.1016/j.jhydrol.2019.03.026.

Corral, C., Velasco, D., Forcadell, D., Sempere-Torres, D., Velasco, E., 2009. Advances in radar-based flood warning systems. In: The EHIMI system and the experience in the Besòs flash-flood pilot basin, in: Flood Risk Management. Research and Practice, p. 309.

CRAHI, 2019. Selection of impacts reported by the media during the DANA event of September 2019 in Spain [WWW Document]. accessed 5.20.21. http://www.crahi.upc.edu/ritter/dana2019/media_impacts.html.

de Bruijn, J.A., de Moel, H., Jongman, B., de Ruiter, M.C., Wagemaker, J., Aerts, J.C.J.H., 2019. A global database of historic and real-time flood events based on social media. Sci. Data 6, 311. https://doi.org/10.1038/s41597-019-0326-9.

de Bruijn, J.A., de Moel, H., Jongman, B., Wagemaker, J., Aerts, J.C.J.H., 2018. TAGGS: Grouping Tweets to Improve Global Geoparsing for Disaster Response. J. Geovisualization Spat. Anal. 2, 1–14. https://doi.org/10.1007/s41651-017-0010-6.

De Moel, H., Van Alphen, J., Aerts, J.C.J.H., 2009. Flood maps in Europe - Methods, availability and use. Nat. Hazards Earth Syst. Sci. 9, 289–301. https://doi.org/10.5194/nhess-9-289-2009.

Deutsche Welle, 2016. Tod und Chaos nach Unwettern in Süddeutschland [WWW Document]. URL https://www.dw.com/de/tod-und-chaos-nach-unwettern-in-süddeutschland/a-19292355 (accessed 7.29.21).

DGPCE, 2019. Informe resumen de la emergencia producida por las graves inundaciones en el sureste, centro peninsular y Baleares (9-15 de septiembre de 2019). Madrid.

Dottori, F., Alfieri, L., Bianchi, A., Skoien, J., Salamon, P., 2021. A new dataset of river flood hazard maps for Europe and the Mediterranean Basin region. Earth Syst. Sci. Data Discuss. 10.5194/essd-2020-313.

Dottori, F., Kalas, M., Salamon, P., Bianchi, A., Alfieri, L., Feyen, L., 2017. An operational procedure for rapid flood risk assessment in Europe. Nat. Hazards Earth Syst. Sci. 17, 1111–1126. https://doi.org/10.5194/nhess-17-1111-2017.

EEA, 2010. Mapping the impacts of recent natural disasters and technological accidents in Europe: an Overwiev of the last decade, EEA Environmental issue report – No. 35. 10.2800/62638.

Emerton, R.E., Stephens, E.M., Pappenberger, F., Pagano, T.C., Weerts, A.H., Wood, A.W., Salamon, P., Brown, J.D., Hjerdt, N., Donnelly, C., Baugh, C.A., Cloke, H.L., 2016. Continental and global scale flood forecasting systems. Wiley Interdiscip. Rev. Water 3, 391–418. https://doi.org/10.1002/wat2.1137.

ERCCa, 2019. DG ECHO Daily Map 17/09/2019 – Spain Floods. https://erccportal.jrc.ec.europa.eu/getdailymap/docId/3045.

[dataset] ERCCb, 2019. EMSR388: Flood in the Southeast of Spain. URL https://emergency.copernicus.eu/mapping/list-of-components/EMSR388.

European Commission, 2015a. EU overview of methodologies used in preparation of Flood Hazard and Flood Risk Maps, Report reference: UC10508/15955-A. 10.2779/204606.

European Commission, 2015b. European Overview Assessment of Member States' reports on Preliminary Flood Risk Assessment and Identification of Areas of Potentially Significant Flood Risk. 10.2779/576456.

European Commission, 2007. Directive 2007/60/EC of the European Parliament and of the Council of 23 October 2007 on the Assessment and Management of Flood Risks, Official Journal of the European Union.

Freire, S., Halkia, M., Pesaresi, M., 2016. GHS population grid, derived from EUROSTAT census data (2011) and ESM R2016. European Commission, Joint Research Centre (JRC) http://data.europa.eu/89h/jrc-ghsl-ghs_pop_eurostat_europe_r2016a (accessed 4.3.20).

García, L., Bermejo, J., Sánchez, J., Guerrero, J., 2020. Dana 2019 y aspectos relativos a la estimación y tratamiento del riesgo asociado a inundaciones, in: Riesgo de Inundación En España: Análisis y Soluciones Para La Generación de Territorios Resilientes. Universidad de Alicante, pp. 143–166.

Gaume, E., Bain, V., Bernardara, P., Newinger, O., Barbuc, M., Bateman, A., Blaškovičová, L., Blöschl, G., Borga, M., Dumitrescu, A., Daliakopoulos, I., Garcia, J., Irimescu, A., Kohnova, S., Koutroulis, A., Marchi, L., Matreata, S., Medina, V., Preciso, E., Sempere-Torres, D., Stancalie, G., Szolgay, J., Tsanis, I., Velasco, D., Viglione, A., 2009. A compilation of data on European flash floods. J. Hydrol. 367, 70–78. https://doi.org/10.1016/j.jhydrol.2008.12.028.

Georgakakos, K.P., 2006. Analytical results for operational flash flood guidance. J. Hydrol. 317, 81–103. https://doi.org/10.1016/j.jhydrol.2005.05.009.

[dataset] Giovando, C., Zia, M., Kalas, M., 2020. Global Exposure Data for Risk Assessment (May 2019 - March 2020) - Project report.

Gourley, J.J., Flamig, Z.L., Hong, Y., Howard, K.W., 2014. Evaluation of past, present and future tools for radar-based flash-flood prediction in the USA. Hydrol. Sci. J. 59, 1377–1389. https://doi.org/10.1080/02626667.2014.919391.

Grillakis, M.G., Koutroulis, A.G., Komma, J., Tsanis, I.K., Wagner, W., Blöschl, G., 2016. Initial soil moisture effects on flash flood generation - A comparison between basins of contrasting hydro-climatic conditions. J. Hydrol. 541, 206–217. https://doi.org/10.1016/j.jhydrol.2016.03.007.

Hapuarachchi, H.A.P., Wang, Q.J., Pagano, T.C., 2011. A review of advances in flash flood forecasting. Hydrol. Process. 25, 2771–2784. https://doi.org/10.1002/hyp.8040.

IGN, . Instituto Geográfico Nacional - Centro de Descargas. accessed 4.1.20. http://centrodedescargas.cnig.es/CentroDescargas/index.jsp. .

Javelle, P., Fouchier, C., Arnaud, P., Lavabre, J., 2010. Flash flood warning at ungauged locations using radar rainfall and antecedent soil moisture estimations. J. Hydrol. 394, 267–274. https://doi.org/10.1016/j.jhydrol.2010.03.032.

Javelle, P., Organde, D., Demargne, J., Saint-Martin, C., de Saint-Aubin, C., Garandeau, L., Janet, B., 2016. Setting up a French national flash flood warning system for ungauged catchments based on the AIGA method. E3S Web Conf. 7, 18010. https://doi.org/10.1051/e3sconf/20160718010i.

Laiolo, P., Gabellani, S., Rebora, N., Rudari, R., Ferraris, L., Ratto, S., Stevenin, H., Cauduro, M., 2014. Validation of the Flood-PROOFS probabilistic forecasting system. Hydrol. Process. 28, 3466–3481. https://doi.org/10.1002/hyp.9888.

Landaverde, E., Sempere-Torres, D., Berenguer, M., 2020. Towards impact-based communication during emergencies: Development of site-specific warning services in Catalonia, in: EGU General Assembly 2020. pp. EGU2020-1011.

Le Bihan, G., Payrastre, O., Gaume, E., Moncoulon, D., Pons, F., 2017. The challenge of forecasting impacts of flash floods: Test of a simplified hydraulic approach and validation based on insurance claim data. Hydrol. Earth Syst. Sci. 21, 5911–5928. https://doi.org/10.5194/hess-21-5911-2017.

LfU, 2016. Sturzfluten- und Hochwasserereignisse Mai/Juni 2016.

Li, H., Lei, X., Shang, Y., Qin, T., 2018. Flash flood early warning research in China. Int. J. Water Resour. Dev. 10.1080/07900627.2018.1435409.

Liechti, K., Panziera, L., Germann, U., Zappa, M., 2013. The potential of radar-based ensemble forecasts for flash-flood early warning in the southern Swiss Alps. Hydrol. Earth Syst. Sci 17, 3853–3869. https://doi.org/10.5194/hess-17-3853-2013.

Martín León, F., 2003. Las gotas frías/DANAs: ideas y conceptos básicos. Madrid.

Merz, B., Kuhlicke, C., Kunz, M., Pittore, M., Babeyko, A., Bresch, D.N., V Domeisen, D.I., Feser, F., Koszalka, I., Kreibich, H., Pantillon, F., Parolai, S., Pinto, J.G., Punge, H.-J., Rivalta, E., Schröter, K., Strehlow, K., Weisse, R., Wurpts, A., 2020. Impact Forecasting to Support Emergency Management of Natural Hazards. Rev. Geophys. 10.1029/2020RG000704.

Munich Re, 2017. Rainstorms over Europe [WWW Document]. accessed 10.21.20. https://www.munichre.com/topics-online/en/climate-change-and-natural-disasters/natural-disasters/floods/rainstorms-europe-2017.html.

Nürnberger Presse, 2016. Obernzenn und Egenhausen versinken im Hochwasser [WWW Document]. accessed 7.29.21. https://www.nordbayern.de/region/bad-windsheim/obernzenn-und-egenhausen-versinken-im-hochwasser-1.5233825.

Paprotny, D., Sebastian, A., Morales-Nápoles, O., Jonkman, S.N., 2018. Trends in flood losses in Europe over the past 150 years. Nat. Commun. 9 https://doi.org/10.1038/s41467-018-04253-1.

Park, S., Berenguer, M., Sempere-Torres, D., 2019. Long-term analysis of gauge-adjusted radar rainfall accumulations at European scale. J. Hydrol. 573, 768–777.

Park, S., Berenguer, M., Sempere-Torres, D., Baugh, C., Smith, P., 2017. Toward seamless high-resolution flash flood forecasting over Europe based on radar nowcasting and NWP: An evaluation with case studies. EGU General Assembly 2017, 2017–12158.

Petrucci, O., Aceto, L., Bianchi, C., Bigot, V., Brázdil, R., Pereira, S., Kahraman, A., Kiliç, Ö., Kotroni, V., Llasat, M.C., Llasat-Botija, M., Papagiannaki, K., Pasqua, A.A., Řehoř, J., Geli, J.R., Salvati, P., Vinet, F., Zêzere, J.L., 2019. Flood fatalities in

Europe, 1980–2018: Variability, features, and lessons to learn. Water (Switzerland) 11. https://doi.org/10.3390/w11081682.
Piper, D., Kunz, M., Ehmele, F., Mohr, S., Mühr, B., Kron, A., Daniell, J., 2016. Exceptional sequence of severe thunderstorms and related flash floods in May and June 2016 in Germany – Part 1: Meteorological background. Nat. Hazards Earth Syst. Sci. 16, 2835–2850. https://doi.org/10.5194/nhess-16-2835-2016.
Priest, S.J., Suykens, C., van Rijswick, H.F.M.W., Schellenberger, T., Goytia, S., Kundzewicz, Z.W., van Doorn-Hoekveld, W.J., Beyers, J.C., Homewood, S., 2016. The European Union approach to flood risk management and improving societal resilience: Lessons from the implementation of the Floods Directive in six European countries. Ecol. Soc. 21 https://doi.org/10.5751/ES-08913-210450.
Raynaud, D., Thielen, J., Salamon, P., Burek, P., Anquetin, S., Alfieri, L., 2015. A dynamic runoff co-efficient to improve flash flood early warning in Europe: Evaluation on the 2013 central European floods in Germany. Meteorol. Appl. 22, 410–418. https://doi.org/10.1002/met.1469.
Ritter, J., Berenguer, M., Corral, C., Park, S., Sempere-Torres, D., 2020. ReAFFIRM: Real-time Assessment of Flash Flood Impacts – a Regional high-resolution Method. Environ. Int. 136, 105375. https://doi.org/10.1016/j.envint.2019.105375.
Ritter, J., Berenguer, M., Dottori, F., Kalas, M., Sempere-Torres, D., 2021b. Compound flood impact forecasting: Integrating fluvial and flash flood impact assessments into a unified system, Hydrol. Earth Syst. Sci. Discuss. [preprint], 10.5194/hess-2021-387.
Ritter, J., Berenguer, M., Park, S., Sempere-Torres, D., 2021a. Rapid flash flood impact assessments at different spatial scales. EGU General Assembly. EGU21-14444.
Saint-Martin, C., Fouchier, C., Javelle, P., Douvinet, J., Vinet, F., 2016. Assessing the exposure to floods to estimate the risk of flood-related damage in French Mediterranean basins, in: E3S Web of Conferences. p. 04013. 10.1051/e3sconf/20160704013.
Sene, K., 2013. Flash Floods. Springer. https://doi.org/10.1007/978-94-007-5164-4.
Silvestro, F., Rebora, N., Ferraris, L., 2011. Quantitative flood forecasting on small- and medium-sized basins: A probabilistic approach for operational purposes. J. Hydrometeorol. 12, 1432–1446. https://doi.org/10.1175/JHM-D-10-05022.1.
Silvestro, F., Rossi, L., Campo, L., Parodi, A., Fiori, E., Rudari, R., Ferraris, L., 2019. Impact-based flash-flood forecasting system: Sensitivity to high resolution numerical weather prediction systems and soil moisture. J. Hydrol. 572, 388–402. https://doi.org/10.1016/j.jhydrol.2019.02.055.
Spitalar, M., Gourley, J.J., Lutoff, C., Kirstetter, P.E., Brilly, M., Carr, N., 2014. Analysis of flash flood parameters and human impacts in the US from 2006 to 2012. J. Hydrol. 519, 863–870. https://doi.org/10.1016/j.jhydrol.2014.07.004.
Taylor, A.L., Kox, T., Johnston, D., 2018. Communicating high impact weather: Improving warnings and decision making processes. Int. J. Disaster Risk Reduct. 30, 1–4. https://doi.org/10.1016/j.ijdrr.2018.04.002.
Terti, G., Ruin, I., Anquetin, S., Gourley, J.J., 2017. A situation-based analysis of flash flood fatalities in the United States. Bull. Am. Meteorol. Soc. 98, 333–345. https://doi.org/10.1175/BAMS-D-15-00276.1.
Thielen, J., Bartholmes, J., Ramos, M.-H., De Roo, A., 2009. The European Flood Alert System-Part 1: Concept and development. Hydrol. Earth Syst. Sci 13, 125–140. https://doi.org/10.5194/hess-13-125-2009.
TUM, 2017. Naturgefahren - von der Sturzflut zur Schwemmholzverklausung. Ereignisanalysen, aktuelle Forschungsvorhaben und Projekte. Technische Universität München.
UNISDR, 2015a. Sendai Framework for Disaster Risk Reduction 2015 - 2030.
UNISDR, 2015b. Global Assessment Report on Disaster Risk Reduction. The Future of Disaster Risk Management, Making Development Sustainable.
Velasco-Forero, C.A., Sempere-Torres, D., Cassiraga, E.F., Gómez-Hernández, J.J., 2009. A non-parametric automatic blending methodology to estimate rainfall fields from rain gauge and radar data. Adv. Water Resour. 32, 986–1002. https://doi.org/10.1016/j.advwatres.2008.10.004.
Versini, P.-A., Berenguer, M., Corral, C., Sempere-Torres, D., 2014. An operational flood warning system for poorly gauged basins: demonstration in the Guadalhorce basin (Spain). Nat. Hazards 71, 1355–1378. https://doi.org/10.1007/s11069-013-0949-7.
Versini, P.-A., Gaume, E., Andrieu, H., 2010. Application of a distributed hydrological model to the design of a road inundation warning system for flash flood prone areas. Nat. Hazards Earth Syst. Sci. 10, 805–817. https://doi.org/10.5194/nhess-10-805-2010.
Vincendon, B., Édouard, S., Dewaele, H., Ducrocq, V., Lespinas, F., Delrieu, G., Anquetin, S., 2016. Modeling flash floods in southern France for road management purposes. J. Hydrol. 541, 190–205. https://doi.org/10.1016/j.jhydrol.2016.05.054.
Ward, P.J., Jongman, B., Salamon, P., Simpson, A., Bates, P., De Groeve, T., Muis, S., De Perez, E.C., Rudari, R., Trigg, M.A., Winsemius, H.C., 2015. Usefulness and limitations of global flood risk models. Nat. Clim. Chang. 10.1038/nclimate2742.
WMO, 2016. WMO Publication No. 9, Volume A, Observing Stations and WMO Catalogue of Radiosondes. URL https://www.wmo.int/pages/prog/www/ois/volume-a/vola-home.htm (accessed 2.25.21).
WMO, 2015. WMO Guidelines on Multi-hazard Impact-based Forecast and Warning Services.
Zappa, M., Rotach, M.W., Arpagaus, M., Dorninger, M., Hegg, C., Montani, A., Ranzi, R., Ament, F., Germann, U., Grossi, G., Jaun, S., Rossa, A., Vogt, S., Walser, A., Wehrhan, J., Wunram, C., 2008. MAP D-PHASE: real-time demonstration of hydrological ensemble prediction systems. Atmos. Sci. Let. 9, 80–87. https://doi.org/10.1002/asl.183.
Zscheischler, J., Martius, O., Westra, S., Bevacqua, E., Raymond, C., 2020. A typology of compound weather and climate events, in: EGU General Assembly 2020. pp. EGU2020-8572. 10.5194/egusphere-egu2020-8572.
Zscheischler, J., Westra, S., Van Den Hurk, B.J.J.M., Seneviratne, S.I., Ward, P.J., Pitman, A., Aghakouchak, A., Bresch, D.N., Leonard, M., Wahl, T., Zhang, X., 2018. Future climate risk from compound events. Nat. Clim. Chang. 8, 469–477. https://doi.org/10.1038/s41558-018-0156-3.